1-2016

# Suppression of NLRP3 inflammasome by γ-tocotrienol ameliorates type 2 diabetes

Yongeun Kim
*University of Nebraska–Lincoln*, ykim41@unl.edu

Wei Wang
*University of Nebraska–Lincoln*

Meshail Okla
*University of Nebraska–Lincoln*

Inhae Kang
*University of Nebraska–Lincoln*

Regis Moreau
*University of Nebraska–Lincoln*, rmoreau2@unl.edu

*See next page for additional authors*

**Authors**

Yongeun Kim, Wei Wang, Meshail Okla, Inhae Kang, Regis Moreau, and Soonkyu Chung

# Suppression of NLRP3 inflammasome by γ-tocotrienol ameliorates type 2 diabetes

Yongeun Kim, Wei Wang, Meshail Okla, Inhae Kang, Regis Moreau, and Soonkyu Chung

Department of Nutrition and Health Sciences, University of Nebraska–Lincoln, Lincoln, NE 68583

Y. Kim and W. Wang contributed equally to this work and are co-first authors.

*Corresponding author* — S. Chung, email schung4@unl.edu

## Abstract

The Nod-like receptor 3 (NLRP3) inflammasome is an intracellular sensor that sets off the innate immune system in response to microbial-derived and endogenous metabolic danger signals. We previously reported that γ-tocotrienol (γT3) attenuated adipose tissue inflammation and insulin resistance in diet-induced obesity, but the underlying mechanism remained elusive. Here, we investigated the effects of γT3 on NLRP3 inflammasome activation and attendant consequences on type 2 diabetes. γT3 repressed inflammasome activation, caspase-1 cleavage, and interleukin (IL) 1β secretion in murine macrophages, implicating the inhibition of NLRP3 inflammasome in the anti-inflammatory and antipyroptotic properties of γT3. Furthermore, supplementation of leptin-receptor KO mice with γT3 attenuated immune cell infiltration into adipose tissue, decreased circulating IL-18 levels, preserved pancreatic β-cells, and improved insulin sensitivity. Mechanistically, γT3 regulated the NLRP3 inflammasome via a two-pronged mechanism: **1)** the induction of A20/TNF-α interacting protein 3 leading to the inhibition of the TNF receptor-associated factor 6/nuclear factor κB pathway and **2)** the activation of AMP-activated protein kinase/autophagy axis leading to the attenuation of caspase-1 cleavage. Collectively, we demonstrated, for the first time, that γT3 inhibits the NLRP3 inflammasome thereby delaying the progression of type 2 diabetes. This study also provides an insight into the novel therapeutic values of γT3 for treating NLRP3 inflammasome-associated chronic diseases.

**Keywords:** inflammation, obesity, vitamin E, insulin signaling, diet and dietary lipids, NOD-like receptor protein 3, A20, caspase 1

γ-Tocotrienol (γT3) is an isomer of unsaturated vitamin E known to exert potent anti-inflammatory functions in various cell types including macrophages, adipocytes, and several cancerous cells (1). There is emerging evidence suggesting that γT3 promotes insulin sensitivity, attenuates adipose inflammation, and decreases hepatosteatosis (2–5). The inhibition of nuclear factor κB (NFKB) signaling has been implicated in the underlying mechanism by which γT3 regulates cellular processes from cell proliferation to insulin sensitization (5–7). However, the fundamental molecular mechanism whereby γT3 modulates inflammation in diverse cell types and mitigates the accompanying pathophysiological sequelae is unknown.

Inflammasomes are multiprotein cytosolic receptors that detect damage signals triggered by invasion of pathogens or by metabolic stresses leading to production of type 1 interferons and proinflammatory cytokines. Excessive activation of inflammasomes is frequently associated with the prevalence of various chronic inflammatory diseases including multiple sclerosis, Alzheimer's disease, atherosclerosis, age-related macular degeneration, and type 1 and 2 diabetes (8). Notably, a critical role of the NOD-like receptor protein 3 (NLRP3) inflammasome has been established in the progression of insulin resistance to type 2 diabetes (9–11). The assembly of inflammasomes is initiated by scaffolding proteins, either NLR (NOD-like receptor proteins) or AIM2 (absent in melanoma 2). It subsequently recruits adaptor protein ASC (apoptosis-associated speck-like protein containing a caspase recruitment domain) and pro-caspase-1. Upon assembly of the inflammasome, caspase-1 becomes active and in turn activates proinflammatory cytokines pro-interleukin (IL)-1β and pro-IL-18 through proteolytic cleavage, resulting in the secretion of IL-1β and IL-18 and cell pyroptosis (reviewed in Ref. 12). Activation of the NLRP3 inflammasome

is regulated by two discrete signaling cues: the priming and assembly of the inflammasome. The priming of NLRP3 inflammasome consists of the transcription of inflammasome components and requires NFKB-mediated transcription of *pro-Il-1β*, *pro-Il-18*, and *Nlrp3* (13). Subsequently, the inflammasome assembles in response to the engagement of pattern recognition receptors by pathogen-associated molecular pattern (PAMP) or damage-associated molecular pattern (DAMP) endogenous signals (sterile inflammation); the latter include FFA, free cholesterol, uric acid, and ATP. One of the key mechanisms by which inflammasome assembly can be repressed is autophagic degradation of these deleterious molecular factors (reviewed in Ref. 14).

Our previous work as well as others has shown that γT3 can block NFKB activation (5–7) and stimulate AMPactivated protein kinase (AMPK) and autophagy in a variety of cell types (15–18). In the present study, we ask whether γT3 represses the NLRP3 inflammasome and associated inflammatory processes in type 2 diabetes by modulating NFKB, AMPK, and autophagy signaling pathways. Using murine macrophages and leptin receptor knockout (*db/db*) mice, we clearly show that γT3 blocks NLRP3 inflammasome activation and ameliorates type 2 diabetes.

## Research Design and Methods

### Chemicals and reagents

γT3 (with 90% purity) was kindly provided by Carotech. γT3 was prepared as previously described (18). Compound C was purchased from Calbiochem. All other chemicals and reagents were purchased from Sigma Chemical Co., unless otherwise stated.

### Animals

All animal experimental procedures were approved by the Institutional Animal Care and Use Committee at the University of Nebraska-Lincoln. Male BKS.Cg-*Dock*7[m+/+]Lepr[db]/J mice (referred to as *db/db* mice) were obtained from Jackson Laboratory. Animals were housed in a specific pathogen-free facility and given free access to food and water. Mice (6 weeks old) were fed a standard AIN93G diet (control) or the AIN93G containing 0.1% (w/w) γT3 for 8 weeks. Mice were given fresh rations daily. Food and water consumption were measured every day for 3 days during the last week of feeding before euthanasia. Individual body weights were measured weekly.

### Preparation of bone marrow-derived macrophages and stimulation for inflammasome

Primary bone marrow cells were isolated from the femurs of 6- to 10-week-old C57BL/6 mice and stimulated to differentiate for 7–10 days in L-cell conditioned medium (CM) as we described previously (5). The resulting differentiated bone marrow-derived macrophages (BMDMs) were pretreated with γT3 or vehicle (DMSO) for 24 h, then primed with lipopolysaccharide (LPS) (100 ng/ml) for 1 h, and stimulated either with nigericin (Ng; 6.5 µM, a $K^+/H^+$ ionophore) for 1 h or palmitate (PA; 400 µM complexed with BSA) for 12 h.

### Pro-IL-1β - *Gaussia* luciferase reporter assay

The J774 macrophages stably expressing pro-IL-1β-*Gaussia* luciferase (iGLuc) fusion construct (**Figure 1A**) were a generous gift from Dr. Hornung (hereafter referred to as iJ774 macrophages)
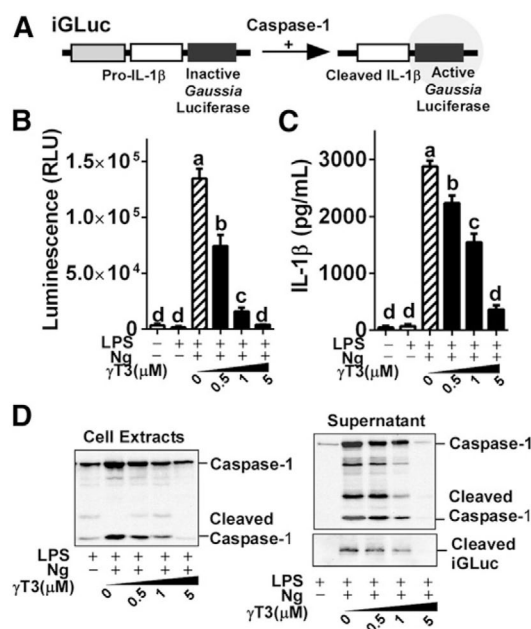


**Figure 1.** γT3 suppressed NLRP3 inflammasome procaspase reporter activity in iJ774 macrophages. iJ774 macrophages were preincubated with γT3 (0–5 µM) for 24 h before LPS priming (100 ng/ml for 1 h) and subsequent Ng stimulation. **A.** Structure of the iGLuc (NLRP3 inflammasome and caspase activity reporter constructs). **B.** Relative GLuc activity was quantified by luminometer. **C.** IL-1β secretion (in medium) quantified by ELISA. Results in B and C are shown as the mean ± SEM (n = 6). Values not sharing a common letter differ significantly (*P* < 0.05) by one-way ANOVA. **D.** Cleavage of caspase-1 in cell extract and supernatant. Results in D are representative of triplicate samples.

(19). iJ774 macrophages were cultured in DMEM supplemented with L-glutamine, sodium pyruvate, and 10% (v/v) FBS (Gibco). To determine *Gaussia* luciferase (GLuc) activity, the BioLux GLuc assay kit (NEB Inc.) was used and read with a Synergy H1 multimode reader (BioTek). The cleavage product of the pro-IL-1β-iGLuc fusion protein was detected in the media by Western blot analysis using anti-GLuc antibody (NEB Inc.).

### Glucose and insulin tolerance tests

A glucose tolerance test (GTT) was performed on fasted (overnight) *db/db* mice by intraperitoneal injection of 10% D-glucose solution [0.5 g/kg body weight (BW)]. Blood glucose levels (mg/dl) were measured at 0, 15, 30, 60, and 120 min after injection using a glucometer (Bayer, Contuor). Plasma insulin levels at basal and 30 min after glucose intraperitoneal injection were determined by ELISA (Crystal Chem). For insulin tolerance test (ITT), fasted (4 h) *db/db* mice were administered 1 U/kg BW of insulin (Novolin R); blood glucose levels were measured at 0, 15, 30, and 60 min after injection.

### Quantitative real-time PCR

Gene expression analysis was performed as described previously (18). Relative gene expression was determined based on the $2^{-\Delta\Delta CT}$ method with normalization of the raw data to either *36b4* or *Gapdh* (see primer sequences in supplementary Table 1). For PCR microarray analysis, $RT^2$ profiler PCR array for mouse inflammasome (PAMM-097ZD) was used according to the manufacturer's instruction (Qiagen). For each treatment, equal amounts of total mRNA obtained from four mice were pooled. The results were analyzed using software provided by Qiagen.

## Immunoblotting, immunoprecipitation, and ELISA

Total cell and tissue extract preparation and Western blot procedures were conducted as we described previously (5). The antibodies recognizing phospho(p)-p38 (Thr180/182), TNF-α interacting protein 3 (A20/TNFAIP3), ATG5, p-IKKα/β (Ser176/180), K63-linkage polyubiquitin, K48-linkage polyubiquitin, p-p44/42-ERK1/2 (Thr202/204), total (t)-ERK, p-AMPKα (Thr 172), t-AMPK, β-actin, LC3, p62, Beclin-1, IκBα, and p-IκBα (Ser32/36) were purchased from Cell Signaling Technology. Antibodies against NLRP3, TNF receptor-associated factor 6 (TRAF6), and caspase-1 (p20) were purchased from R&D Systems, Santa Cruz Biotechnology, and AdipoGen, respectively. For the immunoprecipitation of ubiquitinated-TRAF6, protein A/G magnetic beads (Pierce) were used according to the manufacturer's instruction. Plasma levels of adiponectin, IL-18, and IL-1β were quantified by using commercial ELISA kits from R&D Systems.

## Isolation of stromal vascular cells and flow cytometric analysis

Epididymal fat pads were collected at the time of necropsy and used for stromal vascular (SV) cell isolation by following the protocol of Orr et al. (20). For cell surface staining, cells were stained for 30 min at room temperature in FCS-PBS buffer (1%) with the following antibodies: FITC-CD4, PE-CD8, and APC/Cy7 CD45 and relative isotypes (BioLegend). SV cells were gated using forward and side scatter characteristics for lymphocytes on the basis of at least 10,000 events using a FACSCalibur™ flow cytometer (BD Biosciences). Data were analyzed using FlowJo software (Treestar).

## Hematoxylin and eosin staining, islet size determination, and insulin staining

Paraffin-embedded epididymal adipose tissues from mice were sectioned (10 µm) for hematoxylin and eosin (H&E) staining. Paraffin-embedded pancreases were serially sectioned (5 µm) at 50 µm intervals and used for H&E staining and insulin immunostaining. For determination of average islet size, ~150–200 islets were counted per mouse pancreas from the six serial sections of H and E-stained paraffin block (using Image J software). For insulin staining, pancreas sections were incubated with a primary insulin antibody (dilution 1:50, Dako), followed by incubation with EnVision-AP™ (Dako) and visualized using a SIGMA-*FAST*™ Fast Red system with hematoxylin counterstaining.

## siRNA transfection

siRNAs (On-Target smart pool) targeting mouse A20 (*Tnfaip3)* or nontargeting siRNA control were transfected into iJ774 macrophages at a final concentration of 100 nM using Dharma-FECT4 transfection reagent (GE Dharmacon). Forty-eight hours after transfection, cells were washed and stimulated as indicated in the figure legends.

## Statistics

The two-tailed Student's *t*-test was used for statistical analyses of two-group comparisons. Multigroup comparisons were performed by a one-way ANOVA followed by Tukey's multiple comparison test. All statistical analyses were performed using Graph-Pad Prism 6 (version 6.02).

## Results

### γT3 **Inhibited NLRP3 inflammasome activation in macrophages**

To test whether γT3 suppresses NRLP3-inflammasome activation, we first performed the iGLuc reporter assay for inflammasome and protease activity (Figure 1A) in iJ774 macrophages. The γT3 (0–5 µM) dose-dependently decreased *Gaussia* luminescence upon Ng stimulation of LPS-primed iJ774 macrophages (Figure 1B). Similarly, IL-1β secretion in the medium decreased gradually with increasing dose of γT3 (Figure 1C). In addition, we observed a stepwise decrease of cleaved caspase-1, a surrogate marker for caspase-1 activation, in both cell extracts and supernatants upon treatment with graded dose of γT3 (Figure 1D). We confirmed these results in primary BMDMs where pretreatment with 1 µM γT3 repressed the secretion of IL-1β and IL-18 in LPS-primed Ng-stimulated cells (**Figure 2A)**. The mRNA levels of *Il-1β*, *Il-18*, and *Nlrp3* were also markedly decreased by γT3 (Figure 2B), suggesting that γT3 suppresses the priming of NLRP3 inflammasome. Additionally, the abundance of NLRP3 protein and caspase-1 cleavage were decreased, whereas LC3II and p-AMPKα (Thr172) were increased by γT3 (Figure 2C). To determine whether γT3 is able to suppress DAMP-triggered inflammasome activation, LPS-primed BMDMs were stimulated with 400 µM of PA. γT3 pretreatment (1 µM) remarkably reduced: 1) the secretion of IL-1β and IL-18 in the medium (Figure 2D); 2) the mRNA levels of *Il-1β*, *Il-18*, and *Nlrp3* (Figure 2E); and 3) the protein abundance of NLRP3 and cleaved caspase-1 (Figure 2F). γT3 concomitantly induced LC3II accumulation and AMPK phosphorylation (Figure 2F) implying that the AMP kinase/autophagy axis was stimulated.

### γT3 **ameliorated the progression of type 2 diabetes in** *db/db* **mice**

To determine the effectiveness of γT3 supplementation in preventing the progression of type 2 diabetes, *db/db* mice were fed either an AIN93G diet devoid of γT3 (control) or an AIN93 diet containing 0.1% γT3 (1 g/kg diet) for 8 weeks. Feeding γT3 to *db/db* mice was associated with the improvement of diabetic hyperphagia (**Figure 3A)** and diabetic thirst (polydipsia) (Figure 3B), and a slight but significant increase in body weight (Figure 3C). Importantly, results show a significant decrease in fasting glucose levels (Figure 3D), but an increase of adiponectin levels (Figure 3E). γT3 also improved glucose disposal during the GTT (Figure 3F). There was no significant change in fasting insulin levels between the two groups. However, 30 min within the GTT, plasma insulin failed to rise in control mice, whereas in γT3-fed mice plasma insulin levels were increased ~2-fold (Figure 3G). During the ITT, the insulin injection (1 U/kg BW) markedly improved glucose clearance to the same extent in both groups of mice (Figure 3H). H&E staining of pancreatic islet cells revealed that the average islet size was significantly larger in γT3-fed mice than in controls (Figure 3I), and the islet size distribution shifted toward larger sizes in γT3-fed mice (Figure 3J). Moreover, the percentage of insulin- positive area per islet was significantly higher in γT3- fed mice than controls (5.9% vs. 2.4%; Figure 3K). The immunostaining of the islets also showed that islet integrity was better preserved in γT3-fed mice with a low degree of immune cell infiltration (Figure 3L). Collectively, these data indicate that γT3 attenuates the loss of pancreatic β-cells and delays the progression of type 2 diabetes in *db/db* mice.
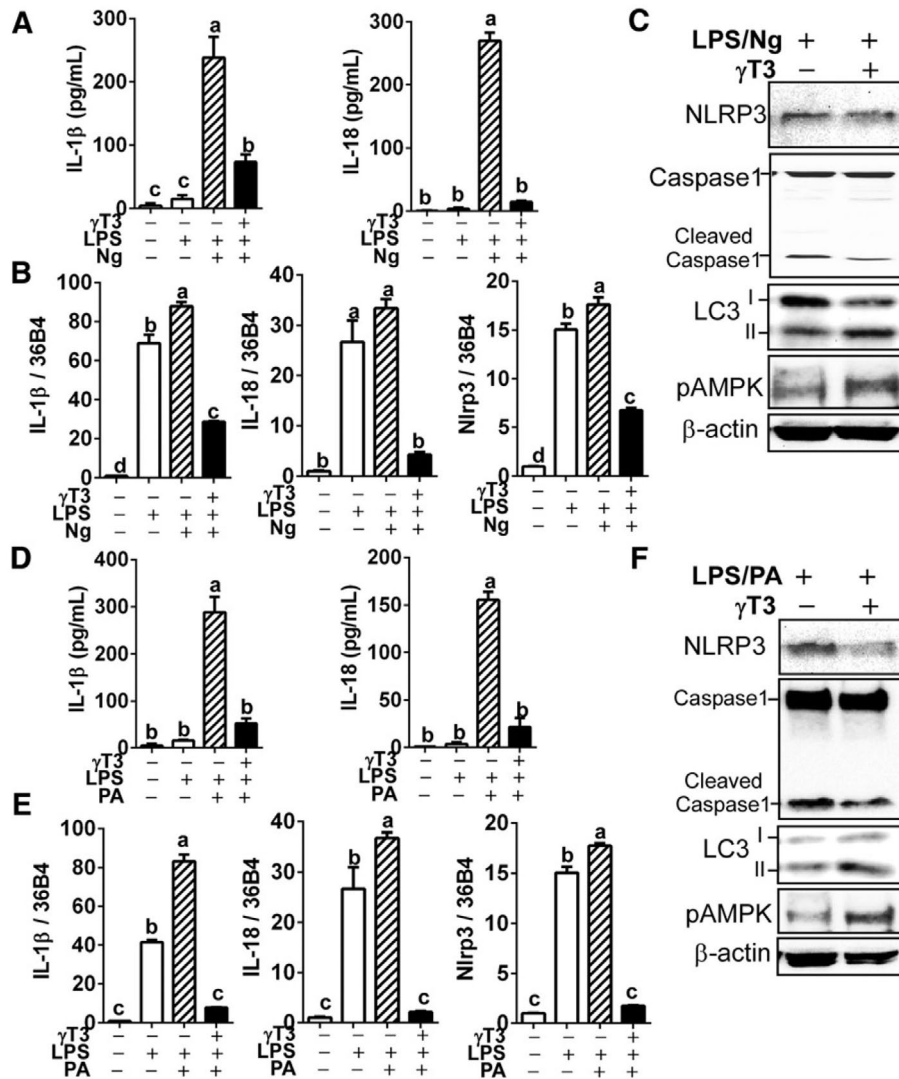
**Figure 2.** γT3 inhibited NLRP3 infl ammasome in BMDMs. BMDMs were preincubated with vehicle (DMSO) or γT3 (1 μM). Inflammasome activation was triggered by either Ng (A–C) or PA (D, E) in LPS-primed BMDMs. IL-1β and IL-18 secreted in culture medium was measured by ELISA (A, D). The mRNA levels of *Il-1β*, *Il-18*, and *Nlrp3* were analyzed by quantitative PCR (qPCR) (B, E). The protein levels of NLRP3, caspase-1, LC3, p-AMPKα (Thr172), and β-actin in cell lysates determined by Western blot (C, F). All data are shown as mean ± SEM in A, B, D, and E (n = 6 per group). Values not sharing a common letter differ significantly (*P* < 0.05) by one-way ANOVA. Results in C and F are representative of triplicate samples.

## γT3 suppressed NLRP3 inflammasome activation in peritoneal macrophages of *db/db* mice

We asked whether the observed improvement of type 2 diabetes sequelae by γT3 was due to the suppression of NLRP3 inflammasome activation and associated inflammatory processes. We found that plasma IL-18 was decreased by ~2-fold in γT3-fed versus control mice (**Figure 4A)**, whereas IL-1β levels were below detection limit in both groups. Next, we isolated the peritoneal macrophages from *db/db* mice fed the experimental diets for 8 weeks to carry out further analysis. Consistent with the results in Figure 1 , the mRNA levels of NFKB target genes, which included *Il-6*, *Tnfα* , *Il-1β* , *Il-18* , *and Nlrp3* , were significantly downregulated in the macrophages of γT3-fed mice (Figure 4B). There was a ~40-fold increase in A20 transcript levels, a negative feedback regulator of NFκB (Figure 4B). The inflammasome 84-gene array revealed that no gene was significantly upregulated by γT3

supplementation. However, six genes (i.e., *Il-12b*, *Nlrp3*, *Nfkbib*, *Nlrc5*, *NLrp4b*, and *Nlrp12*) were differentially downregulated >2-fold in the macrophages of γT3-fed mice (Figure 4C ; also see supplementary Table 2). Western blot analyses showed that the macrophages of γT3-fed mice had less phosphorylated MAP kinase (p-ERK and p38), more IκBα and A20/TNFAIP3, and less NLRP3 and cleaved caspase-1 (Figure 4D).

We also investigated the role of γT3 in autophagy in peritoneal macrophages of *db/db* mice. p-AMPKα (Thr 172) as well as markers of autophagic activation, including Beclin-1, autophagy protein 5 (ATG5), and LC3II, were markedly increased by γT3, whereas p62 was decreased by γT3 (Figure 4E). Because p62 is degraded in autolysosome, p62 levels are inversely correlated with autophagic flux. To confirm that the autophagic flux was stimulated by γT3, BMDMs were treated with chloroquine (CQ), a lysosomal degradation in-
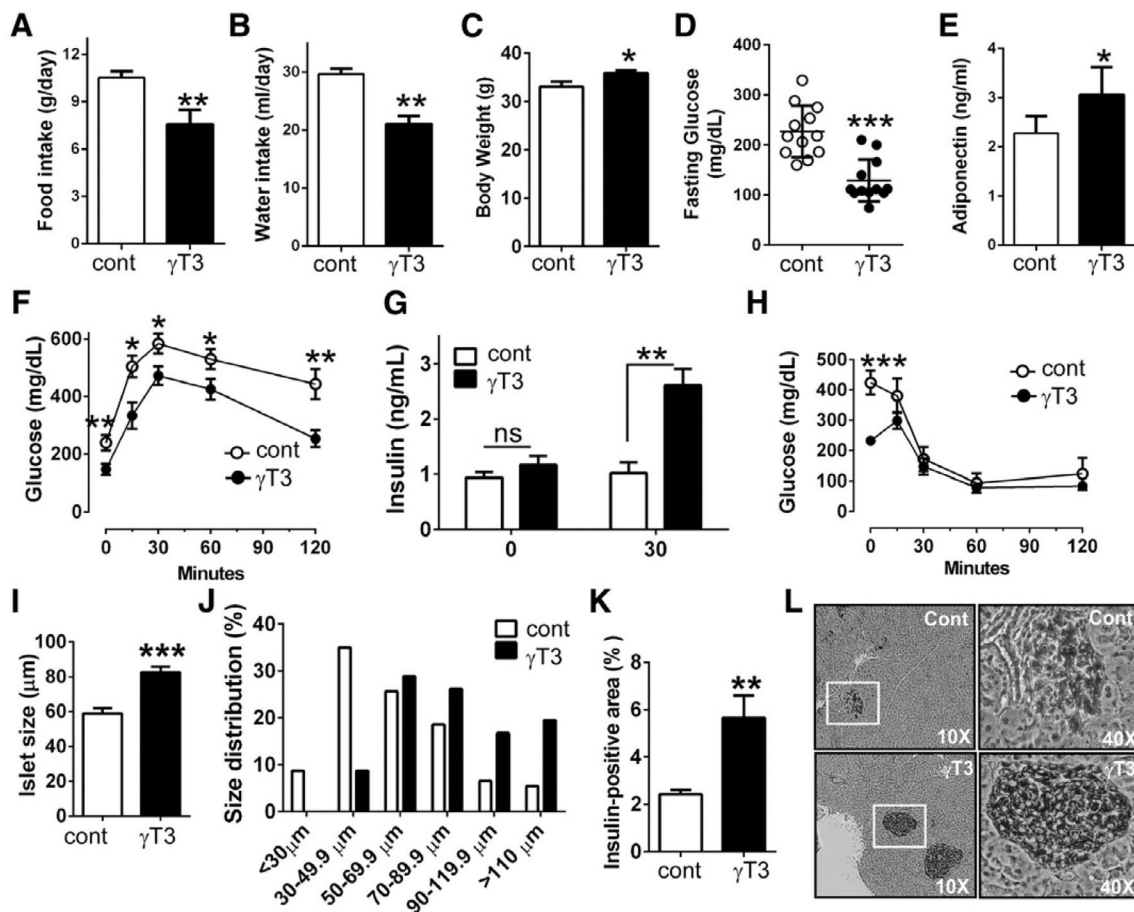
**Figure 3.** γT3 ameliorated the progression of type 2 diabetes in *db/db* mice. Male *db/db* mice were fed with either an AIN93G control diet devoid of γT3 or an AIN93G diet containing 0.1% γT3 for 8 weeks (n = 12 mice per group). **A.** Food intake. **B.** Water intake. **C.** Body weight. **D.** Fasting glucose levels. **E.** Adiponectin levels (ELISA). **F.** GTT. **G.** Plasma insulin levels at 0 and 30 min after intraperitoneal glucose injection were quantified by ELISA. **H.** ITT. **I.** Average size of islets of Langerhans. **J.** Relative size distribution of the pancreatic islets. **K.** Percentage of insulin-positive area/pancreas area. **L.** Representative images of insulin-positive islet area after immunohistochemical staining of insulin (n = 5). All data are shown as mean ± SEM. * $P < 0.05$ ; ** $P < 0.01$ ; *** $P < 0.001$ by Student's *t*-test.

hibitor. γT3 (but not control) led to LC3II accumulation and p62 degradation in CQ-treated BMDMs (Figure 4F) implying that γT3 coregulates autophagosome formation and inflammasome activation. Taken together, these data revealed that γT3 decreased NLRP3 inflammasome activation in macrophages of *db/db* mice.

**γT3 decreased immune cell infiltration into white adipose tissue and preserved insulin sensitivity**

The impact of γT3-mediated suppression of NLRP3 inflammasome activation on adipose tissue inflammation was further investigated in epididymal white adipose tissue (WAT) of *db/db* mice. H&E staining revealed that γT3 supplementation significantly reduced immune cell infiltration into WAT (**Figure 5A)**. Flow cytometric analysis of the SV fractions showed that total macrophage infiltration (F4/80+) was decreased by ~30% in γT3-fed versus control mice (12.3% vs. 8.3%; Figure 5B). In addition, *Cd11c* gene expression was substantially decreased in the WAT of γT3-fed mice (Figure 5C). In accordance with the anti-inflammatory role of γT3 in peritoneal macrophages (Figure 4C), feeding γT3 to *db/db* mice decreased the mRNA levels of *Il-1β*, *Il-18*, and *Nlrp3* but raised

those of *A20* in WAT (Figure 5D). Flow cytometry data revealed that the total leukocytes (CD45+) and cytotoxic T-cell populations (CD45+/CD8+) were significantly decreased in the WAT of γT3-fed mice compared with control WAT (Figure 5E).

Next, we examined whether γT3 modulates NLRP3 inflammasome activation in WAT. Our results showed that γT3 supplementation decreased NLRP3 expression, ERK phosphorylation, and caspase-1 cleavage, but increased protein levels of IκBα and A20 in epididymal WAT (Figure 5F). Furthermore, the WAT of γT3-fed mice exhibited higher AMPK phosphorylation (Thr172) and Beclin-1 and LC3II abundance, but lower abundance of p62 compared with control mice (Figure 5G), collectively suggesting activation of the AMPK/autophagy axis by γT3.

To assess whether γT3 could preserve insulin sensitivity of adipocytes from the deleterious effects of IL-1β, primary mouse adipocytes differentiated from mesenchymal stem cells were first cultured with or without γT3 (1 μM). Then adipocyte cultures were exposed to the IL-1β-containing CM obtained from LPS/Ng-treated iJ774 (Figure 5H , left). The insulin-stimulated Akt phosphorylation was significantly reduced following exposure to the CM (Figure 5H , lane 5), un-
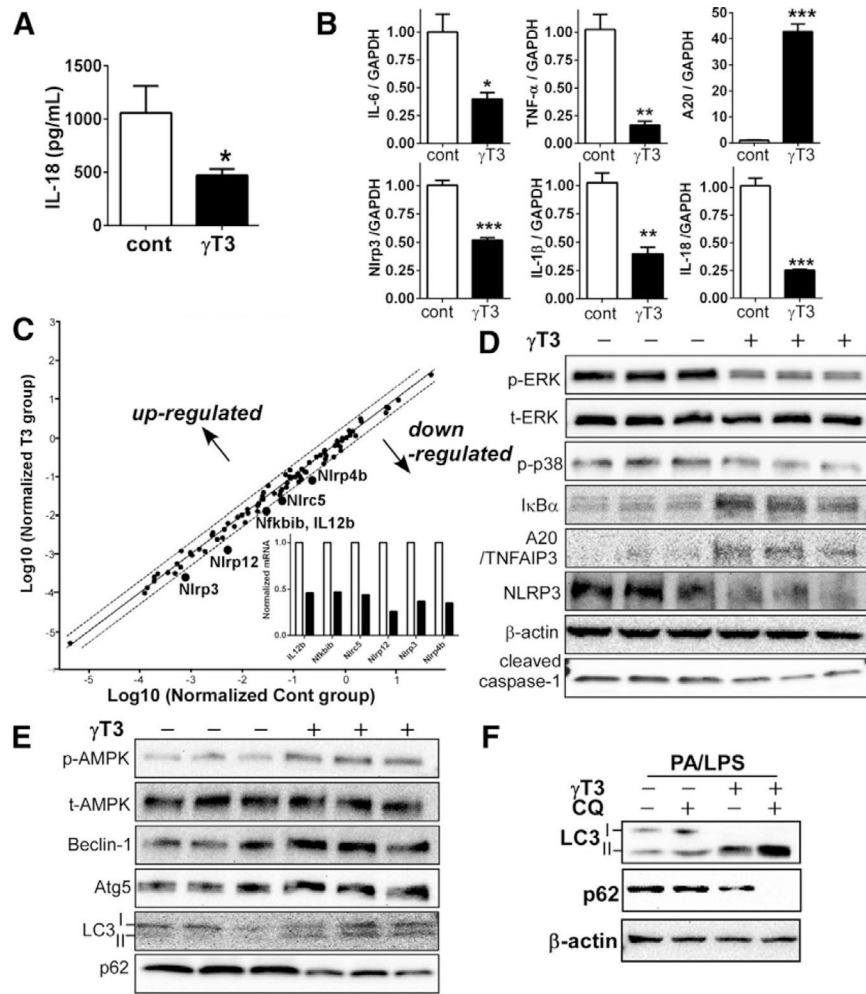
**Figure 4.** Feeding γT3 to *db/db* mice repressed the formation of NLRP3 inflammasomes in peritoneal macrophages. **A.** IL-18 levels (ELISA) in blood plasma collected from control and γT3-fed *db/db* mice (n = 6). **B.** The mRNA expression of *Il-6*, *Tnfα*, *Il-1β*, *Il-18*, *A20*, and *Nlrp3* analyzed by qPCR in isolated peritoneal macrophages (n = 6). **C.** Microarray analysis of mouse inflammasome (84 genes) by qPCR. Pooled mRNA (n = 4 per group) was used for analysis. Target genes positioned outside the space defined by the broken lines are differentially expressed by at least 2-fold. Insert. Fold change of downregulated genes (open bar, control macrophages; closed bar, γT3-fed macrophages). **D.** Western blot analysis of p-ERK, t-ERK, p-p38, IκBα, A20, NLRP3, and cleaved caspase-1. **E.** Western blot analysis for p-AMPK and t-AMPK, and autophagyrelated protein expression of Beclin-1, Atg5, LC3, and p62 (see supplementary Figure 1 for quantification). **F.** BMDMs were stimulated for inflammasome formation by PA/LPS for 12 h. CQ (10 μM, an autophagy inhibitor) was added 3 h before harvest. Protein levels of LC3I/II, p62, and β-actin were determined by Western blot (n = 3). Data in A and B are expressed as mean ± SEM. * *P* < 0.05 ; ** *P* < 0.01 ; *** *P* < 0.001.

less the adipocytes had received γT3 (Figure 5H , lane 6). Collectively, these data demonstrate that γT3 reduced NFKB and NLRP3 inflammasome activation in WAT resulting in attenuation of adipose tissue inflammation and preservation of insulin sensitivity.

**γT3 blocked NFKB-mediated priming of the inflammasome**

NFκB activation is a critical step for the priming of the inflammasomes. Based on multiple observations that γT3 increased A20 expression (Figs. 4, 5), we hypothesized that γT3 inhibits NFKB signaling pathway via activation of A20, an ubiquitination-editing enzyme. We further hypothesized that A20 activation hinders the ubiquitination of TRAF6. The formation of a polyubiquitin chain (K63-Ub) on TRAF6 is critical for TRAF6-mediated phosphorylation and activation of IKK. Following activation, IKK phosphorylates IκB, which undergoes

proteosomal degradation thereby allowing NFκB to dimerize into its active form (21). To test these hypotheses, BMDMs were pretreated with or without γT3 (1 μM) and then stimulated with LPS, and mRNAs and proteins were collected over a 3 h time course. We found that *Il-1β* mRNA levels were inversely associated with those of *A20* (**Figure 6A)**. The elevation of A20 protein abundance induced by γT3 coincided with: 1) the decrease of p-IκB kinase (IKK) α/β, p-ERK, and p-IκBα; 2) the reappearance of IκBα; and 3) the disappearance of TRAF6, suggesting a negative feedback of A20 on TRAF6/IKK/NFκB signaling (Figure 6B).

It has been shown that A20 can transfer TRAF6-bound Ub from residue K63 to K48 thereby causing the proteasomal degradation of TRAF6 (22). Thus, we performed immunoprecipitation to determine K63- versus K48-Ub status of TRAF6. As opposed to the study by Muroi and Tanamoto (22), inhibition of proteasomal degradation by MG132 failed to rescue
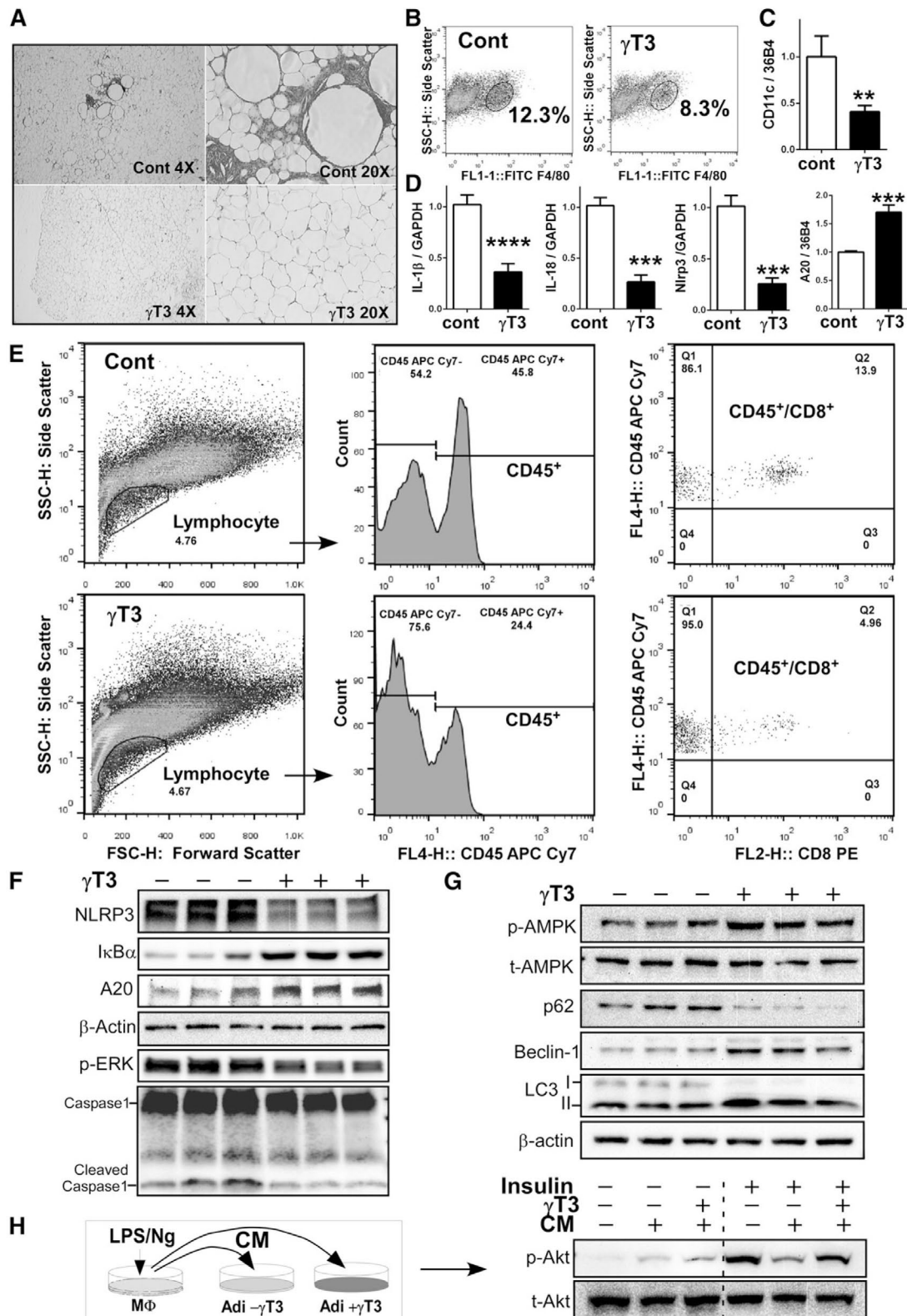
**Figure 5.** γT3 supplementation regulated innate immune system and insulin sensitivity in WAT. Epididymal adipose tissues were isolated from the control and γT3-fed *db/db* mice. **A.** H and E staining. **B.** Flow cytometric determination of F4/80⁺ population from adipose SV fraction (representative flow cytogram of four mice per group). **C.** *Cd11c* gene expression (n = 6). **D.** mRNA expression *Il-1β, Il-18, Nlrp3*, and *A20* (n = 6). Data are expressed as mean ± SEM. * *P* < 0.05 ; ** *P* < 0.01 ; *** *P* < 0.001. **E.** CD45⁺ and CD45⁺CD8⁺ T-cell fractions by flow cytometry (representative flow cytogram of four mice per group). **F.** Western blot analysis of NLRP3, IκBα , A20/TNFAIP3, cleaved caspase-1, and β-actin (loading control). **G.** Western blot analysis of p-AMPK, t-AMPK, p62, Beclin-1, LC3, and β-actin. Each lane represents epididymal WAT from different animals (see supplementary Figure 2 for quantification). **H.** Inflammasome formation was stimulated by LPS/ Ng in iJ774 cells. Primary murine adipocytes were preincubated with γT3 before receiving the CM of LPS/Ng-treated iJ774 (left). Insulin (100 nM)-stimulated levels of p-Akt and t-Akt were determined by Western blot analysis (right).

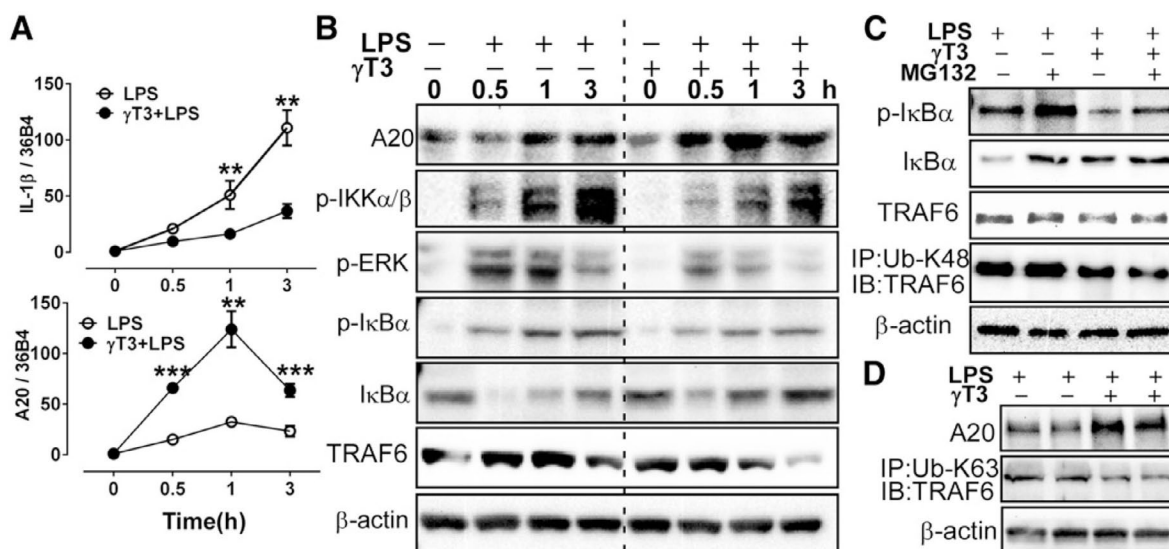**Figure 6.** γT3 blocked NFκB-mediated priming of the inflammasome in BMDMs. BMDMs were pretreated with vehicle (–) or γT3 (+) for 24 h. **A, B.** Cells were stimulated with LPS (100 ng/ml) at t = 0 h, then total RNA and cellular proteins were extracted at 0, 0.5, 1, and 3 h. **A.** Temporal changes in mRNA levels of *Il-1β* and *A20* by qPCR. **B.** Temporal changes in protein abundance of A20, p-IKK, p-ERK, p-IκBα, IκBα, TRAF6, and β-actin by Western blot analysis. **C.** BMDMs were pretreated with proteasomal degradation inhibitor MG132 (50 μM) prior to LPS stimulation (1 h). Protein levels of p-IKBA, IκBα, TRAF6, and β-actin were determined by Western blot. Cell extracts were immunoprecipitated (IP) with K48 ubiquitination antibody (Ub-K48) then immunoblotted (IB) with antibodies against TRAF6. **D.** BMDMs were stimulated with LPS for 1 h. Cell extracts were immunoprecipitated (IP) with K63 ubiquitination antibody (Ub-K63) then immunoblotted (IB) with antibodies against TRAF6. Data are shown as mean ± SEM. ** *P* < 0.01 ; *** *P* < 0.001.

the γT3-mediated decrease of TRAF6 or to increase K48-Ub of TRAF6 (Figure 6C). Similarly, γT3 also lowered K63-Ub of TRAF6 compared with controls (Figure 6D). Taken together, we posit that A20 induction by γT3 inhibited the ubiquitination of both the K48 and K63 residues of TRAF6 and promoted TRAF6 nonproteasomal degradation, leading to early blockage of the NFKB signaling pathway and repression of inflammasome priming.

### Inhibition of A20 and AMPK activation altered IL-1β secretion and caspase-1 cleavage by γT3

To determine whether AMPK mediates γT3's inhibition of the inflammasome, we treated iJ774 macrophages with Compound C (10 μM), a chemical inhibitor of AMPK. Results showed that Compound C partially reversed γT3-dependent decreases in IL-1β secretion (**Figure 7A**), caspase-1 cleavage (Figure 7B , top), and iGLuc activity (Figure 7B , bottom). To ascertain the contribution of A20 induction by γT3 in the lowering of IL-1β secretion and caspase-1 activation, A20 was knocked down in iJ774 macrophages using siRNAs . As expected, the silencing of A20 effectively decreased γT3-mediated A20 induction but did not reverse γT3-mediated blockage of caspase-1 cleavage (Figure 7C). Although total IL-1β levels were significantly increased in siA20-transfected cells versus siControl cells, the extent to which γT3 attenuated IL-1β secretion was not significantly different between siA20 and siControl cells (Δ of columns 1 and 2 vs. Δ of columns 3 and 4; Figure 7D). Taken together, our results suggest that 1) AMPK mediates the blockage of caspase-1 cleavage afforded by γT3, 2) A20 downregulates NFκB-mediated pro-

duction of IL-1β , and 3) γT3 can inhibit IL-1β production independently of A20.

### Discussion

The activation of the NLRP3 inflammasome is positively associated with the prevalence of type 2 diabetes. Consequently, targeting the inhibition of NLRP3 inflammasome is an attractive strategy against type 2 diabetes. In this study, we addressed the question of whether γT3, an unsaturated form of vitamin E, is effective in suppressing the NLRP3 inflammasome and mitigating the pathophysiological consequences of inflammation in a mouse model of type 2 diabetes. Our results showed that γT3 inhibits the NLRP3 inflammasome activity by two-pronged mechanism: 1) the blockage of inflammasome priming and 2) the impediment of inflammasome activation. To our knowledge, this is the first study to characterize the role of γT3 in inhibiting the NLRP3 inflammasome and show that, by acting through the inflammasome, γT3 dietary supplementation can improve insulin resistance in mice.

Intense research is currently being devoted to the discovery of chemical inhibitors of the NLRP3 inflammasome (23), blocking agents of the IL-1β signaling such as IL-1R (IL-1 receptor) antagonist (24), and neutralizing antibodies (25, 26). Although, there is growing evidence that nutrition is a critical modulator of the inflammasome, few attempts have been made to inhibit the NLRP3 inflammasome through diet. For instance, elevated levels of circulating FFAs were shown to activate the NLRP3 inflammasome and weaken insulin sensitivity (27, 28). In contrast, ω-3 FA (29) and MUFAs (30) have
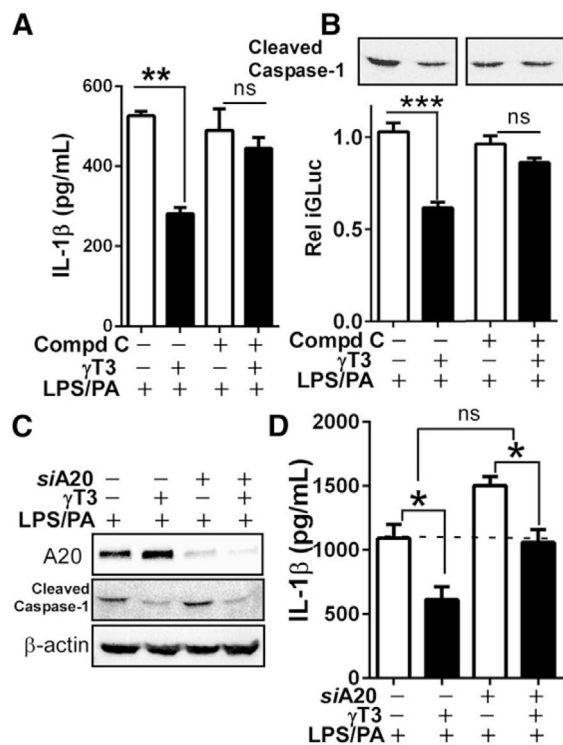
**Figure 7.** AMPK and A20 contributed to γT3-mediated lowering of IL-1β secretion. iJ774 macrophages were treated with Compound C (10 μM) to inhibit AMPK (A–C) or transfected with either A20- targeting siRNA (siA20+) or nontargeting siRNA (siA20–) followed by LPS/PA stimulation for 12 h (C, D). **A.** Secreted IL-1β was measured by ELISA (n = 6). **B.** Relative GLuc activity of iGLuc (bottom) and caspase-1 cleavage (top). **C.** Western blot analysis of A20, cleaved caspase-1, and β-actin (representative of triplicate samples). **D.** Secreted IL-1β was measured by ELISA (n = 6). The dotted line indicates the basal IL-1β level of siCont cells primed with LPS/PA. All data are expressed as mean ± SEM. * P < 0.05 ; ** P < 0.01 ; *** P < 0.001 ; ns, nonsignificant.

been shown to curtail NLRP3 inflammasome activation. In this study, we report on the previously unrecognized function of γT3 [at physiologically relevant concentration (1)] as a potent negative regulator of the NLRP3 inflammasome. Our data clearly show that γT3 inhibited the NLRP3 inflammasome in three macrophage models [i.e., iJ774 macrocytic cells (Figure 1), primary BMDMs (Figure 2), and peritoneal macrophages freshly isolated from *db/db* mice (Figure 4)]. In addition, the suppression of NLPR3 inflammasomes by γT3 was evident upon stimulation of PAMP with Ng, and of DAMP with PA (Figure 2). We also found that γT3 altered the NLR-subset inflammasome, but not the AIM2-scaffold inflammasome, the adaptor protein ASC, or the other caspases (Figure 4C), suggesting that γT3 has therapeutic potential against metabolic diseases where the NLRP3 inflammasome is implicated, such as obesity, atherosclerosis, and type 2 diabetes (8).

In the obese, the chronic stimulation of Toll-like receptor 4 by FAs has been shown to activate the NLRP3 inflammasome of macrophages residing in the adipose tissue and provoke the massive influx of immune cells into WAT (27, 31). Here, we investigated the potential mitigating properties of dietary γT3 on the inflammatory and immunological consequences

of obesity toward glycemia, insulinemia, and WAT remodeling. To that end, we determined the composition of NLRP3 inflammasomes, the extent of immune cell infiltration, and insulin sensitivity. We found that the lowering of NLRP3 inflammasome in the WAT of γT3-fed mice (Figure 5F) was associated with the lowering of cytotoxic CD8⁺ T cells and macrophages in WAT (Figure 5A, B), and with the amelioration of insulin resistance (Figs. 3, 5H).

The destruction of pancreatic β-cells and impairment of insulin production are hallmarks of late-stage type 2 diabetes (32, 33). Because of a lack of specimens, we were unable to determine whether the protection of β cells afforded by γT3 (Figure 3I–L) was due to the blockage of inflammasome formation within the islets or the insensitivity of β cells to the deleterious effects of IL-1β paracrine signaling. We are currently investigating whether γT3 inhibits the inflammasome of macrophages residing in islets or the inflammasome of β cells themselves, or both.

Mechanistically, we had anticipated that γT3 would inhibit the priming of NLRP3 inflammasome based on γT3's intrinsic ability to suppress NFκB (5). However, we did not anticipate that γT3 would augment A20 induction, an ubiquitin-editing enzyme (34). Single nucleotide polymorphisms in the *Tnfaip3/A20* are associated with increased susceptibility to chronic inflammatory diseases (35, 36). Deletion of A20 has been shown to cause hypersensitivity to TNF-α due to the constitutive activation of NFκB, leading to premature death (37). In addition, an inverse correlation between diabetes incidence and A20 mRNA levels was found in patients with both type 1 and type 2 diabetes (38). In our study, multiple lines of evidence demonstrated that A20 is augmented by γT3 to mitigate the priming of the NLRP3 inflammasome (Figs. 4, 6, and 7). Recently, Wang et al. (39) have reported that γT3 causes A20 induction via regulation of sphingolipid metabolism. It is presently unknown whether alterations to sphingolipid metabolism by γT3 affected NLRP3 inflammasome activity in our study. Nonetheless, the work by Wang et al. corroborates our claim that γT3 protects against abnormal stimulation of the innate immune system in part through the upregulation of A20 and feedback inhibition of priming of the NLRP3 inflammasome. Indeed, A20 silencing with siRNA did not completely reverse γT3's inhibition of IL-1β secretion (Figure 7C, D), suggesting that A20 activation is important but not sufficient, and full inhibition of NLRP3 inflammasome necessitates the coordinated involvement of additional factors. One of these factors may be autophagy because Matsuzawa et al. (40) reported that A20 activation and autophagy cooperate in T-cell survival.

Autophagy regulates the fate of inflammasomes by engulfing PAMP and DAMP signals (41, 42). We clearly demonstrated that γT3 activates AMPK and autophagy (Figs. 2, 4, and 5). We further showed that the inhibition of AMPK with Compound C almost completely reversed γT3's suppression of NLRP3 inflammasome and caspase-1 cleavage, indicating that AMPK activation is critically important in the mechanism of γT3 (Figure 7). Further research exploring the cross-talks between the A20 and AMPK/autophagy signaling pathways is needed to fully understand the precise mechanism by which γT3 suppresses NLRP3 inflammasome activation.

Most tocotrienol dietary supplements are provided as mixed formulations of α-, γ-, and δ-tocotrienols, with the exception of tocotrienol supplmentation isolated from annatto seeds, which contain >90% of δ-tocotrienol. The bioavailability of γT3 has been shown to vary in humans depending on the tocotrienol composition of the dietary source, the target population, and the study design (reviewed in Ref. 43). Tocotrienols circulate in blood bound to lipoproteins, in particular to HDL particles, suggesting that the plasma lipoprotein profile affects tocotrienol metabolism. Due to the low binding affinity of tocotrienols for the α-tocopherol transfer protein, the transfer of tocotrienols to HDL particles must occur via alternative, yet to be identified pathways (44, 45). The tocotrienol-rich fraction supplementations are considered safe. They obtained the GRAS (Generally Recognized as Safe) designation from the Food and Drug Administration. Based on a recent review by Podszun et al. (46), there is no clear evidence that high doses of vitamin E (>300 mg/day), either as tocotrienols or tocopherols, cause adverse effects in either animals or humans. However, we note that a meta-analysis of human studies with vitamin E raised some concerns with regard to high-dose vitamin E supplementation, which may have adverse effects when consumed with certain drugs, such as aspirin (47). Despite some uncertainties regarding the metabolism of tocotrienols, multiple clinical studies support their beneficial effects against metabolic diseases (48). By showing that γT3 inhibits the NLRP3 inflammasome and considering that the innate immune response plays a central role in metabolic disorders, our study may provide a possible explanation for some of the clinical positive outcomes of tocotrienol supplementation (8).

In summary, the critical role of the NLRP3 inflammasome in the pathophysiology of insulin resistance was confirmed in human studies (49, 50). Hence, by revealing that γT3 supplementation blunts NLRP3 inflammasome activity and delays the progression of type 2 diabetes, our present work has clinical relevance. Although further investigations in human subjects are necessary to validate the therapeutic applicability of our work, we herein present seminal evidence that γT3 is an anti-inflammatory vitamin by inhibiting the NLRP3 inflammasome in macrophages.

## References

1. Jiang, Q. 2014. Natural forms of vitamin E: Metabolism, antioxidant, and anti-inflammatory activities and their role in disease prevention and therapy. *Free Radic. Biol. Med.* **72:** 76–90.

2. Burdeos, G. C., K. Nakagawa, F. Kimura, and T. Miyazawa. 2012. Tocotrienol attenuates triglyceride accumulation in HepG2 cells and F344 rats. *Lipids.* **47:** 471–481.

3. Siddiqui, S., H. Ahsan, M. R. Khan, and W. A. Siddiqui. 2013. Protective effects of tocotrienols against lipid-induced nephropathy in experimental type-2 diabetic rats by modulation in TGF-beta expression. *Toxicol. Appl. Pharmacol.* **273:** 314–324.

4. Haghighat, N., M. Vafa, S. Eghtesadi, I. Heidari, A. Hosseini, and A. Rostami. 2014. The effects of tocotrienols added to canola oil on microalbuminuria, inflammation, and nitrosative stress in patients with type 2 diabetes: A randomized, double-blind, placebo-controlled trial. *Int. J. Prev. Med.* **5:** 617–623.

5. Zhao, L., I. Kang, X. Fang, W. Wang, M. A. Lee, R. R. Hollins, M. R. Marshall, and S. Chung. 2015. Gamma-tocotrienol attenuates highfat diet-induced obesity and insulin resistance by inhibiting adipose inflammation and M1 macrophage recruitment. *Int. J. Obes. (Lond.).* **39:** 438–446.

6. Ahn, K. S., G. Sethi, K. Krishnan, and B. B. Aggarwal. 2007. Gamma-tocotrienol inhibits nuclear factor-kappaB signaling pathway through inhibition of receptor-interacting protein and TAK1 leading to suppression of antiapoptotic gene products and potentiation of apoptosis. *J. Biol. Chem.* **282:** 809–820.

7. Wang, Y., and Q. Jiang. 2013. gamma-Tocotrienol inhibits lipopolysaccharide-induced interleukin-6 and granulocyte colonystimulating factor by suppressing C/EBPbeta and NF-kappaB in macrophages. *J. Nutr. Biochem.* **24:** 1146–1152.

8. Ozaki, E., M. Campbell, and S. L. Doyle. 2015. Targeting the NLRP3 inflammasome in chronic inflammatory diseases: current perspectives. *J. Inflamm. Res.* **8:** 15–27.

9. Stienstra, R., C. J. Tack, T. D. Kanneganti, L. A. Joosten, and M. G. Netea. 2012. The inflammasome puts obesity in the danger zone. *Cell Metab.* **15:** 10–18.

10. Stienstra, R., J. A. van Diepen, C. J. Tack, M. H. Zaki, F. L. van de Veerdonk, D. Perera, G. A. Neale, G. J. Hooiveld, A. Hijmans, I. Vroegrijk, et al. 2011. Inflammasome is a central player in the induction of obesity and insulin resistance. *Proc. Natl. Acad. Sci. USA.* **108:** 15324–15329.

11. Vandanmagsar, B., Y. H. Youm, A. Ravussin, J. E. Galgani, K. Stadler, R. L. Mynatt, E. Ravussin, J. M. Stephens, and V. D. Dixit. 2011. The NLRP3 inflammasome instigates obesity-induced inflammation and insulin resistance. *Nat. Med.* **17:** 179–188.

12. Latz, E., T. S. Xiao, and A. Stutz. 2013. Activation and regulation of the inflammasomes. *Nat. Rev. Immunol.* **13:** 397–411.

13. Bauernfeind, F. G., G. Horvath, A. Stutz, E. S. Alnemri, K. MacDonald, D. Speert, T. Fernandes-Alnemri, J. Wu, B. G. Monks, K. A. Fitzgerald, et al. 2009. Cutting edge: NF-kappaB activating pattern recognition and cytokine receptors license NLRP3 inflammasome activation by regulating NLRP3 expression. *J. Immunol.* **183:** 787–791.

14. Martins, J. D., J. Liberal, A. Silva, I. Ferreira, B. M. Neves, and M. T. Cruz. 2015. Autophagy and inflammasome interplay. *DNA Cell Biol.* **34:** 274–281.

15. Rickmann, M., E. C. Vaquero, J. R. Malagelada, and X. Molero. 2007. Tocotrienols induce apoptosis and autophagy in rat pancreatic stellate cells through the mitochondrial death pathway. *Gastroenterology.* **132:** 2518–2532.

16. Tiwari, R. V., P. Parajuli, and P. W. Sylvester. 2015. gamma-Tocotrienolinduced endoplasmic reticulum stress and autophagy act concurrently to promote breast cancer cell death. *Biochem. Cell Biol.* **93:** 306–320.

17. Wu, S. J., G. Y. Huang, and L. T. Ng. 2013. gamma-Tocotrienol induced cell cycle arrest and apoptosis via activating the Bax-mediated mitochondrial and AMPK signaling pathways in 3T3–L1 adipocytes. *Food Chem. Toxicol.* **59:** 501–513.

18. Zhao, L., J. H. Ha, M. Okla, and S. Chung. 2014. Activation of autophagy and AMPK by gamma-tocotrienol suppresses the adipogenesis in human adipose derived stem cells. *Mol. Nutr. Food Res.* **58:** 569–579.

19. Bartok, E., F. Bauernfeind, M. G. Khaminets, C. Jakobs, B. Monks, K. A. Fitzgerald, E. Latz, and V. Hornung. 2013. iGLuc: A luciferase-based inflammasome and protease activity reporter. *Nat. Methods.* **10:** 147–154.

20. Orr, J. S., A. J. Kennedy, and A. H. Hasty. 2013. Isolation of adipose tissue immune cells. *J. Vis. Exp.* **75:** 50707.

21. Boone, D. L., E. E. Turer, E. G. Lee, R. C. Ahmad, M. T. Wheeler, C. Tsui, P. Hurley, M. Chien, S. Chai, O. Hitotsumatsu, et al. 2004. The ubiquitin-modifying enzyme A20 is required for termination of Toll-like receptor responses. *Nat. Immunol.* **5:** 1052–1060.

22. Muroi, M., and K. Tanamoto. 2012. IRAK-1-mediated negative regulation of Toll-like receptor signaling through proteasome-dependent downregulation of TRAF6. *Biochim. Biophys. Acta.* **1823:** 255–263.

23. Coll, R. C., A. A. Robertson, J. J. Chae, S. C. Higgins, R. Munoz-Planillo, M. C. Inserra, I. Vetter, L. S. Dungan, B. G. Monks, A. Stutz, et al. 2015. A small-molecule inhibitor of the NLRP3 inflammasome for the treatment of inflammatory diseases. *Nat. Med.* **21:** 248–255.

Seifert, T. Mandrup-Poulsen, and M. Y. Donath. 2007. Interleukin-1-receptor antagonist in type 2 diabetes mellitus. *N. Engl. J. Med.* **356:** 1517–1526.

25. Dinarello, C. A., and J. W. van der Meer. 2013. Treating inflammation by blocking interleukin-1 in humans. *Semin. Immunol.* **25:** 469–484.

26. Jesus, A. A., and R. Goldbach-Mansky. 2014. IL-1 blockade in autoinflammatory syndromes. *Annu. Rev. Med.* **65:** 223–244.

27. Wen, H., D. Gris, Y. Lei, S. Jha, L. Zhang, M. T. Huang, W. J. Brickey, and J. P. Ting. 2011. Fatty acid-induced NLRP3-ASC inflammasome activation interferes with insulin signaling. *Nat. Immunol.* **12:** 408–415.

28. Reynolds, C. M., F. C. McGillicuddy, K. A. Harford, O. M. Finucane, K. H. Mills, and H. M. Roche. 2012. Dietary saturated fatty acids prime the NLRP3 inflammasome via TLR4 in dendritic cell-simplications for diet-induced insulin resistance. *Mol. Nutr. Food Res.* **56:** 1212–1222.

29. Yan, Y., W. Jiang, T. Spinetti, A. Tardivel, R. Castillo, C. Bourquin, G. Guarda, Z. Tian, J. Tschopp, and R. Zhou. 2013. Omega-3 fatty acids prevent inflammation and metabolic disorder through inhibition of NLRP3 inflammasome activation. *Immunity.* **38:** 1154–1163.

30. Finucane, O. M., C. L. Lyons, A. M. Murphy, C. M. Reynolds, R. Klinger, N. P. Healy, A. A. Cooke, R. C. Coll, L. McAllan, K. N. Nilaweera, et al. 2015. Monounsaturated fatty acid-enriched high-fat diets impede adipose NLRP3 inflammasome-mediated IL-1beta secretion and insulin resistance despite obesity. *Diabetes.* **64:** 2116–2128.

31. Nishimura, S., I. Manabe, M. Nagasaki, K. Eto, H. Yamashita, M. Ohsugi, M. Otsu, K. Hara, K. Ueki, S. Sugiura, et al. 2009. CD8+ effector T cells contribute to macrophage recruitment and adipose tissue inflammation in obesity. *Nat. Med.* **15:** 914–920.

32. Potter, K. J., C. Y. Westwell-Roper, A. M. Klimek-Abercrombie, G. L. Warnock, and C. B. Verchere. 2014. Death and dysfunction of transplanted beta-cells: Lessons learned from type 2 diabetes? *Diabetes.* **63:** 12–19.

33. Weir, G. C., and S. Bonner-Weir. 2004. Five stages of evolving beta-cell dysfunction during progression to diabetes. *Diabetes.* **53 (Suppl. 3):** S16–S21.

34. Vereecke, L., R. Beyaert, and G. van Loo. 2009. The ubiquitin-editing enzyme A20 (TNFAIP3) is a central regulator of immunopathology. *Trends Immunol.* **30:** 383–391.

35. Mele, A., J. R. Cervantes, V. Chien, D. Friedman, and C. Ferran. 2014. Single nucleotide polymorphisms at the TNFAIP3/A20 locus and susceptibility/resistance to inflammatory and autoimmune diseases. *Adv. Exp. Med. Biol.* **809:** 163–183.

36. Vereecke, L., R. Beyaert, and G. van Loo. 2011. Genetic relationships between A20/TNFAIP3, chronic inflammation and autoimmune disease. *Biochem. Soc. Trans.* **39:** 1086–1091.

37. Lee, E. G., D. L. Boone, S. Chai, S. L. Libby, M. Chien, J. P. Lodolce, and A. Ma. 2000. Failure to regulate TNF-induced NFkappaB and cell death responses in A20-deficient mice. *Science.* **289:** 2350–2354.

38. Cheng, L., D. Zhang, Y. Jiang, W. Deng, Q. Wu, X. Jiang, and B. Chen. 2014. Decreased A20 mRNA and protein expression in peripheral blood mononuclear cells in patients with type 2 diabetes and latent autoimmune diabetes in adults. *Diabetes Res. Clin. Pract.* **106:** 611–616.

39. Wang, Y., N. Y. Park, Y. Jang, A. Ma, and Q. Jiang. 2015. Vitamin E gamma-tocotrienol inhibits cytokine-stimulated NF-kappaB activation by induction of anti-inflammatory A20 via stress adaptive response due to modulation of sphingolipids. *J. Immunol.* **195:** 126–133.

40. Matsuzawa, Y., S. Oshima, M. Takahara, C. Maeyashiki, Y. Nemoto, M. Kobayashi, Y. Nibe, K. Nozaki, T. Nagaishi, R. Okamoto, et al. 2015. TNFAIP3 promotes survival of CD4 T cells by restricting MTOR and promoting autophagy. *Autophagy.* **11:** 1052–1062.

41. Wang, Y., Y. B. Li, J. J. Yin, Y. Wang, L. B. Zhu, G. Y. Xie, and S. H. Pan. 2013. Autophagy regulates inflammation following oxidative injury in diabetes. *Autophagy.* **9:** 272–277.

42. Yuk, J. M., and E. K. Jo. 2013. Crosstalk between autophagy and inflammasomes. *Mol. Cells.* **36:** 393–399.

43. Fu, J. Y., H. L. Che, D. M. Tan, and K. T. Teng. 2014. Bioavailability of tocotrienols: Evidence in human studies. *Nutr. Metab. (Lond).* **11:** 5.

44. Khosla, P., V. Patel, J. M. Whinter, S. Khanna, M. Rakhkovskaya, S. Roy, and C. K. Sen. 2006. Postprandial levels of the natural vitamin E tocotrienol in human circulation. *Antioxid. Redox Signal.* **8:** 1059–1068.

45. Fairus, S., R. M. Nor, H. M. Cheng, and K. Sundram. 2006. Postprandial metabolic fate of tocotrienol-rich vitamin E differs significantly from that of γ-tocopherol. *Am. J. Clin. Nutr.* **84:** 835–842.

46. Podszun, M., and J. Frank. 2014. Vitamin E-drug interactions: Molecular basis and clinical relevance. *Nutr. Res. Rev.* **27:** 215–231.

47. Bjelakovic, G., D. Nikolova, L. L. Gluud, R. G. Simonetti, and C. Gluud. 2007. Mortality in randomized trials of antioxidant supplements for primary and secondary prevention: Systematic review and meta-analysis. *J. Am. Med. Assoc.* **297:** 842–857.

48. Aggarwal, B. B., C. Sundaram, S. Prasad, and R. Kannappan. 2010. Tocotrienols, the vitamin E of the 21st century: Its potential against cancer and other chronic diseases. *Biochem. Pharmacol.* **80:** 1613–1631.

49. Esser, N., L. L'homme, R. A. De, L. Kohnen, A. J. Scheen, M. Moutschen, J. Piette, S. Legrand-Poels, and N. Paquot. 2013. Obesity phenotype is related to NLRP3 inflammasome activity and immunological profile of visceral adipose tissue. *Diabetologia.* **56:** 2487–2497.

50. Lee, H. M., J. J. Kim, H. J. Kim, M. Shong, B. J. Ku, and E. K. Jo. 2013. Upregulated NLRP3 inflammasome activation in patients with type 2 diabetes. *Diabetes.* **62:** 194–204.

# Supplemental Data

**Suppression of NLRP3 inflammasome by gamma-tocotrienol ameliorates type 2 diabetes**

Yongeun Kim[1,2], Wei Wang[1,2], Meshail Okla[1], Inhae Kang[1], and Regis Moreau[1], Soonkyu Chung[1*]

[1]Department of Nutrition and Health Sciences, University of Nebraska-Lincoln, Lincoln, NE, 68583

**Supplementary Table 1. Primer sequences for qPCR**

| Gene | Forward (5'→3') | Reverse (5'→3') |
|---|---|---|
| 36B4 | GGATCTGCTGCATCTGCTTG | GGCGACCTGGAAGTCCAACT |
| CD11c | CTGGATAGCCTTTCTTCTGCT | GCACACTGTGTCCGAACT |
| F4/80 | CTTTGGCTATGGGCTTCCAGTC | GCAAGGAGGACAGAGTTTATCGTG |
| GAPDH | CATGGCCTTCCGTGTTCCTA | GCGGCACGTCAGATCCA |
| IL-18 | GACAGCCTGTGTTCGAGGAT | TGGATCCATTTCCTCAAAGG |
| IL-1β | GTCACAAGAAACCATGGCACAT | GCCCATCAGAGGCAAGGA |
| IL-6 | CTGCAAGAGACTTCCATCCAGTT | AGGGAAGGCCGTGGTTGT |
| NLRP3 | ATGCTGCTTCGACATCTCCT | AACCAATGCGAGATCCTGAC |
| TNFα | GGCTGCCCCGACTACGT | ACTTTCTCCTGGTATGAGATAGCAAAT |
| A20 | AAACCAATGGTGATGGAAACTG | GTTGTCCCATTCGTCATTCC |

**Supplemental Table2**. Fold changes of mouse inflammasome related genes by qPCR microarray in pooled peritoneal macrophages of *db/db* mice after 12 weeks of γT3 supplementation.

| Abbreviation | Description | Fold |
|---|---|---|
| Aim2 | Absent in melanoma 2 | 1.1196 |
| Bcl2 | B-cell leukemia/lymphoma 2 | 0.7285 |
| Bcl2l1 | Bcl2-like 1 | 0.7049 |
| Birc2 | Baculoviral IAP repeat-containing 2 | 0.7128 |
| Birc3 | Baculoviral IAP repeat-containing 3 | 0.9341 |
| Card6 | Caspase recruitment domain family, member 6 | 1.0997 |
| Casp1 | Caspase 1 | 1.219 |
| Casp12 | Caspase 12 | 1.0918 |
| Casp8 | Caspase 8 | 1.1355 |
| Ccl12 | Chemokine (C-C motif) ligand 12 | 1.4828 |
| Ccl5 | Chemokine (C-C motif) ligand 5 | 0.8065 |
| Ccl7 | Chemokine (C-C motif) ligand 7 | 1.2402 |
| Cd40lg | CD40 ligand | 0.7801 |
| Cflar | CASP8 and FADD-like apoptosis regulator | 0.7188 |
| Chuk | Conserved helix-loop-helix ubiquitous kinase | 1.1336 |
| Ciita | Class II transactivator | 0.6468 |
| Ctsb | Cathepsin B | 0.6855 |
| Cxcl1 | Chemokine (C-X-C motif) ligand 1 | 0.5347 |
| Cxcl3 | Chemokine (C-X-C motif) ligand 3 | 0.7117 |
| Fadd | Fas (TNFRSF6)-associated via death domain | 0.6265 |
| Hsp90aa1 | Heat shock protein 90, alpha (cytosolic), class A member 1 | 1.0587 |
| Hsp90b1 | Heat shock protein 90, beta (Grp94), member 1 | 0.6649 |
| Ifnb1 | Interferon beta 1, fibroblast | 1.0196 |
| Ifng | Interferon gamma | 1.3048 |
| Ikbkb | Inhibitor of kappaB kinase beta | 0.9313 |
| Ikbkg | Inhibitor of kappaB kinase gamma | 1.4305 |
| Il12a | Interleukin 12A | 0.857 |
| Il12b | Interleukin 12B | **0.4649** |
| Il18 | Interleukin 18 | 0.556 |
| Il1b | Interleukin 1 beta | 0.5773 |
| Il33 | Interleukin 33 | 0.7311 |
| Il6 | Interleukin 6 | 0.9015 |
| Irak1 | Interleukin-1 receptor-associated kinase 1 | 1.1393 |
| Irf1 | Interferon regulatory factor 1 | 0.5369 |
| Irf3 | Interferon regulatory factor 3 | 1.0506 |
| Irf4 | Interferon regulatory factor 4 | 0.9299 |
| Map3k7 | Mitogen-activated protein kinase kinase kinase 7 | 0.9728 |

| Mapk1 | Mitogen-activated protein kinase 1 | 1.5487 |
|---|---|---|
| Mapk11 | Mitogen-activated protein kinase 11 | 1.1737 |
| Mapk12 | Mitogen-activated protein kinase 12 | 0.7196 |
| Mapk13 | Mitogen-activated protein kinase 13 | 1.751 |
| Mapk3 | Mitogen-activated protein kinase 3 | 0.9884 |
| Mapk8 | Mitogen-activated protein kinase 8 | 0.5988 |
| Mapk9 | Mitogen-activated protein kinase 9 | 0.8816 |
| Mefv | Mediterranean fever | 0.7729 |
| Myd88 | Myeloid differentiation primary response gene 88 | 1.032 |
| Naip1 | NLR family, apoptosis inhibitory protein 1 | 0.877 |
| Naip5 | NLR family, apoptosis inhibitory protein 5 | 0.8364 |
| Nfkb1 | Nuclear factor of kappa light polypeptide gene enhancer in B-cells 1, p105 | 0.9456 |
| Nfkbia | Nuclear factor of kappa light polypeptide gene enhancer in B-cells inhibitor, alpha | 0.9229 |
| Nfkbib | Nuclear factor of kappa light polypeptide gene enhancer in B-cells inhibitor, beta | **0.4697** |
| Nlrc4 | NLR family, CARD domain containing 4 | 1.0828 |
| Nlrc5 | NLR family, CARD domain containing 5 | **0.4488** |
| Nlrp12 | NLR family, pyrin domain containing 12 | **0.265** |
| Nlrp1a | NLR family, pyrin domain containing 1A | 1.3147 |
| Nlrp3 | NLR family, pyrin domain containing 3 | **0.3759** |
| Nlrp4b | NLR family, pyrin domain containing 4B | **0.3513** |
| Nlrp4e | NLR family, pyrin domain containing 4E | 1.8363 |
| Nlrp5 | NLR family, pyrin domain containing 5 | 1.3688 |
| Nlrp6 | NLR family, pyrin domain containing 6 | 1.0314 |
| Nlrp9b | NLR family, pyrin domain containing 9B | 0.9511 |
| Nlrx1 | NLR family member X1 | 0.9174 |
| Nod1 | Nucleotide-binding oligomerization domain containing 1 | 0.9508 |
| Nod2 | Nucleotide-binding oligomerization domain containing 2 | 0.9979 |
| P2rx7 | Purinergic receptor P2X, ligand-gated ion channel, 7 | 1.033 |
| Panx1 | Pannexin 1 | 1.6384 |
| Pea15a | Phosphoprotein enriched in astrocytes 15A | 0.8337 |
| Pstpip1 | Proline-serine-threonine phosphatase-interacting protein 1 | 1.1191 |
| Ptgs2 | Prostaglandin-endoperoxide synthase 2 | 0.6537 |
| Pycard | PYD and CARD domain containing | 1.0224 |
| Rela | V-rel reticuloendotheliosis viral oncogene homolog A (avian) | 0.5653 |
| Ripk2 | Receptor (TNFRSF)-interacting serine-threonine kinase 2 | 0.9019 |
| Stk30 | Serine/threonine kinase 30 | 1.0472 |
| Sugt1 | SGT1, suppressor of G2 allele of SKP1 (S. cerevisiae) | 1.0874 |
| Tab1 | TGF-beta activated kinase 1/MAP3K7 binding protein 1 | 0.6241 |
| Tab2 | TGF-beta activated kinase 1/MAP3K7 binding protein 2 | 0.8919 |

| | | |
|---|---|---|
| Tirap | Toll-interleukin 1 receptor (TIR) domain-containing adaptor protein | 1.1931 |
| Tnf | Tumor necrosis factor | 0.5095 |
| Tnfsf11* | Tumor necrosis factor (ligand) superfamily, member 11 | 2.4853 |
| Tnfsf14 | Tumor necrosis factor (ligand) superfamily, member 14 | 0.963 |
| Tnfsf4 | Tumor necrosis factor (ligand) superfamily, member 4 | 0.6236 |
| Traf6 | Tnf receptor-associated factor 6 | 0.8629 |
| Txnip | Thioredoxin interacting protein | 0.7104 |
| Xiap | X-linked inhibitor of apoptosis | 1.1982 |
| Actb | Actin, beta | 0.928 |
| B2m | Beta-2 microglobulin | 0.8583 |
| Gapdh | Glyceraldehyde-3-phosphate dehydrogenase | 1.0041 |
| Gusb | Glucuronidase, beta | 0.7756 |
| Hsp90ab1 | Heat shock protein 90 alpha (cytosolic), class B member 1 | 0.9962 |

*Ct cycle >30

# Supplemental Figure 1

**A**



**B**
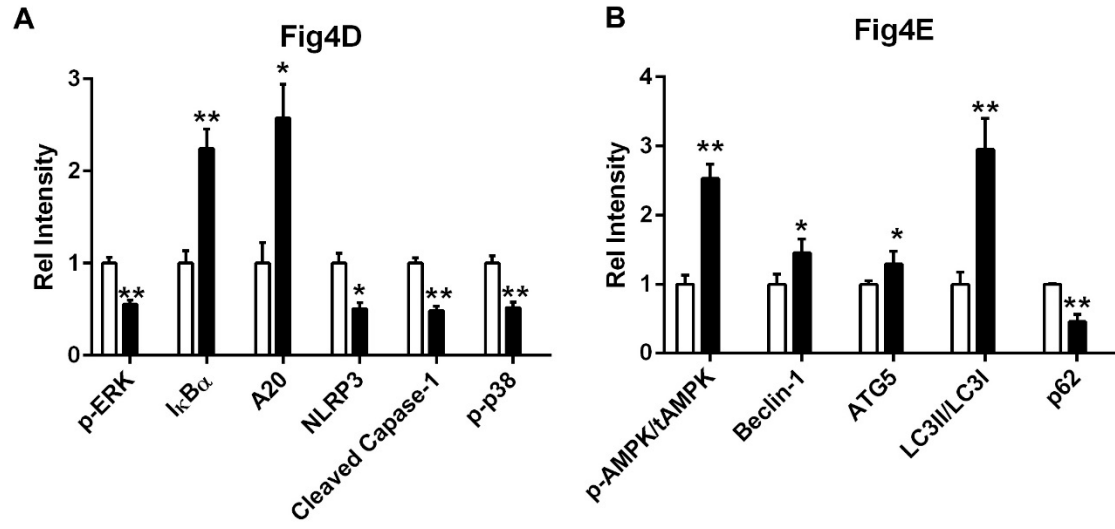


**Supplemental Fig1**. Band densitometry of Fig 4D (A) and Fig 4E (B) was quantified with Image J software and normalized to β-actin with the exception of p-ERK that was normalized to t-ERK, LC3II that was normalized to LC3I, and p-AMPK that was normalized to t-AMPK. Open bars correspond to peritoneal macrophages isolated from mice fed control diet. Closed bars correspond to peritoneal macrophages isolated from mice fed 0.1% γT3. *P<0.05, **P<0.001 by Student's *t*-test.

## Supplemental Figure 2

**A**

### Fig5F



**B**
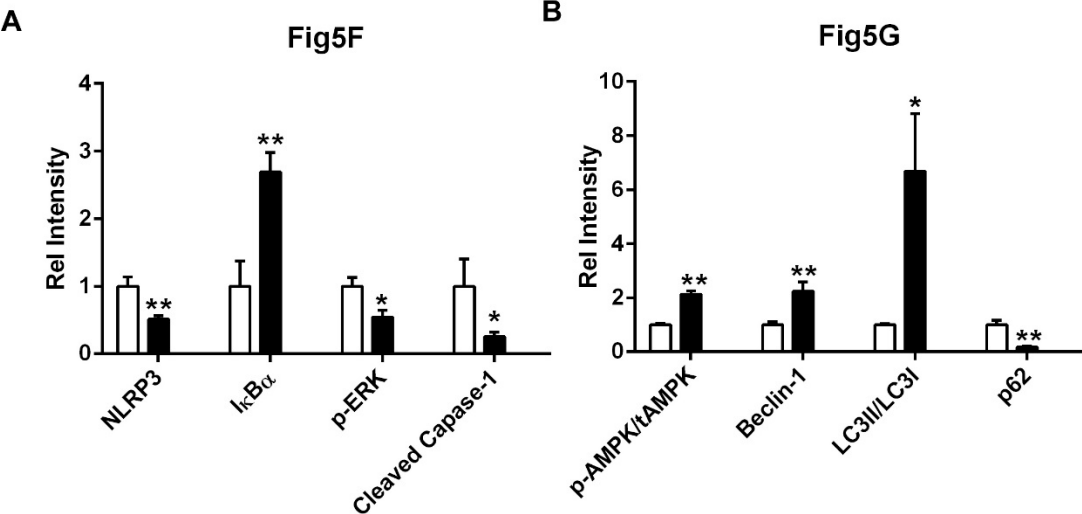
### Fig5G



**Supplemental Fig2**. Band densitometry of Fig 5F (A) and Fig 5G (B) was determined with

Image J software and normalized to β-actin with the exception of p-ERK that was normalized to

t-ERK, LC3II that was normalized to LC3I, and p-AMPK that was normalized to t-AMPK. Open

bars correspond to WAT of mice fed control diet. Closed bars correspond to WAT of mice fed

0.1% γT3. *P<0.05, **P<0.001 by Student t-test.